

# Stability and Noise of Electric Current from Field Emitters for Nano Manufacturing

King-Fu Hui\*, R. Ryan Vallance†, and M. Pinar Mengüç‡

\*Mechanical Engineering, University of Kentucky  
015 Ralph G. Anderson Building, Lexington, KY 40506, USA

†Precision Systems Laboratory, The George Washington University  
738 Phillips Hall, 801 22<sup>nd</sup> St., N.W., Washington, DC, 20052, USA  
Tel: +1-202-994-9830; Fax: +1-202-994-0238. Email: vallance@gwu.edu

‡Mechanical Engineering, University of Kentucky  
269 Ralph G. Anderson Building, Lexington, KY, 40506, USA

## Introduction

Substantial interest in the use of carbon nanotubes (CNTs) as electron sources or field emitters was stimulated by the earliest reports of their exceptional field emission behavior [1,2], which results from their high aspect ratio, electrical conductivity, and inertness. An important criterion for their practical usefulness as an electron emitter in devices such as electron microscopy and vacuum micro-electronic devices is their stability and noise characteristics. Such a CNT-based emitter may suit several nano manufacturing and metrology applications where electron beams are required. Here, we are particularly interested in using the emitter for nano machining, in which the electron beam from the emitter provides a concentrated source of thermal energy [3].

The emission of electrons by quantum-mechanical tunneling in field emission requires high vacuum and high electric field at the tip of the emitter. The surface where the electrons are emitted is typically small ( $< 1000 \text{ nm}^2$ ) and scales with tip size, which makes the emission current susceptible to transient conditions, especially due to adsorption or desorption of adsorbates at the emitting sites.

As demonstrated in prior reports of field emission from individual CNTs [4,5], the emitted current density  $J$  [ $\text{A}/\text{m}^2$ ] is adequately modeled by the Fowler-Nordheim (FN) theory [6] given in Eq. (1) with work function  $\phi$  [eV], local electric field at the CNT tip  $E$  [V/nm], and the constants  $a$  and  $b$  equal to  $1.541 \times 10^{-6} \text{ A} \cdot \text{eV} \cdot \text{V}^{-2}$  and  $6.831 \times 10^9 \text{ eV}^{-3/2} \cdot \text{V} \cdot \text{m}^{-1}$ , respectively.

$$J = \frac{aE^2}{\phi^2(y)} \exp\left[-\frac{b\phi^{3/2}}{E} v(y)\right] \quad (1)$$

The dimensionless functions  $t(y)$  and  $v(y)$  result from including the image charge effect into the surface potential barrier. These slowly varying functions are approximated by Eqs. (2) and (3) for  $y$  given by Eq. (4).

$$t(y) = 1 + 0.1156y^{1.40} \quad (2)$$

$$v(y) = 1 - 1.0125y^{1.71} \quad (3)$$

$$y = 3.7947 \times 10^{-5} \frac{E^{1/2}}{\phi} \quad (4)$$

The experimentally measurable quantities, current  $I$  [A] and voltage  $V$  [V], are related to the FN equation by assuming that  $J = I/A_{\text{eff}}$  and  $E = \beta V/d$ .  $A_{\text{eff}}$  [ $\text{m}^2$ ] is the effective emitting area,  $\beta$  is the field enhancement factor, and  $d$  [m] is the gap distance measured from the tip of CNT to the anode surface.

Fransen [7] studied the long-term stability of the emission current from a CNT field emitter by sampling every few minutes over a period of several weeks. Though such investigations are extremely important for applications requiring long-term stability, it is not informative for variability over just a few seconds or minutes. Others [8,9] used field emission microscopy to image changes in field emission patterns with a phosphor screen while also measuring emission current. This enables correlation of the dynamic changes in the emission sites to the fluctuations in the recorded emission current.

In this paper, the noise and stability of a CNT field emitter was studied using an apparatus with a nanopositioning stage that allowed for fine adjustments to the electrode gap. The transient current is separated into high frequency (noise) and low frequency (stability) components in the frequency domain. Then the noise and stability were characterized with statistical parameters such as mean, root-mean-square (rms), skewness, and kurtosis. This approach proves useful in comparing relative amounts of noise and stability under different operating conditions.

## Experiment

The CNT field emitter (cathode) used in the experiment was prepared by attaching a multiwall carbon nanotube, synthesized by the chemical vapor

deposition (CVD) using xylene and ferrocene, to the tip of a sharpened  $\varnothing$  150  $\mu\text{m}$  tungsten wire as shown in the scanning electron micrograph of Fig. 1. The CNT of  $\sim \varnothing$  100 nm protrudes about 600 nm from the sharpened tip. The anode is a  $\varnothing$  125  $\mu\text{m}$  cleaved optical fiber that was coated with copper along its cylindrical surface to connect with a gold layer deposited on the fiber's cleaved end.

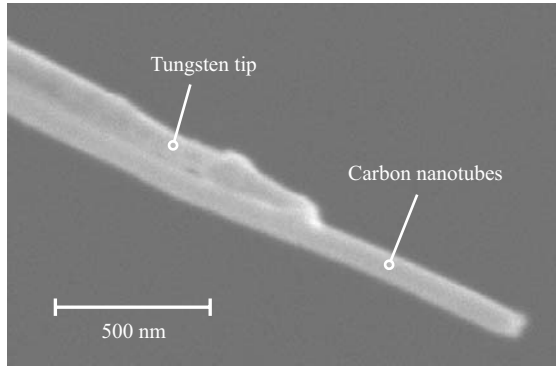


Fig. 1 CNT field Emitter

Our experiments are performed in an ultra-high-vacuum (UHV) chamber with vacuum base pressure of about  $10^{-8}$  mbar ( $\sim 10^{-8}$  Torr) using the apparatus and instrumentation illustrated in Fig. 2, which consists of a nanopositioning stage, a high gain transimpedance amplifier, and a low-noise high voltage power supply. A PC controls the experiments and records measured data.

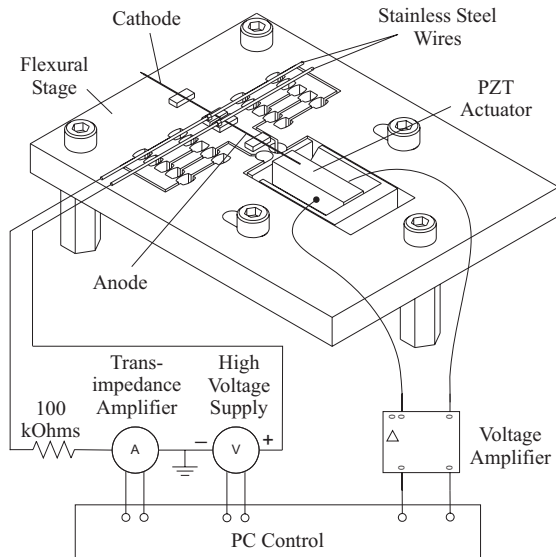


Fig. 2 Experimental setup

The anode and cathode are passively aligned by pressing them into two grooves that are micro-machined into quartz substrates. This arrangement establishes a sharp cathode aimed at a much larger

anode that is flat and smooth to within  $\sim 10$  nm as estimated by scanning white light interferometry. We use stainless steel wires to preload the electrodes into the grooves and provide electrical contact with each electrode. The gap distance of the electrodes is adjusted to about 35  $\mu\text{m}$ .

The cathode is held at ground potential, and a positive voltage is applied to the anode using a high-voltage power supply (Bertan Model 230-03R), which is remotely controlled by the PC. The emission current is measured with a transimpedance amplifier (Keithley, Model 428) that has adjustable gains from  $10^3$  to  $10^{11}$  V/A.

All the measurements in this study were recorded at a sampling frequency of 20 kHz. To reduce aliasing in the recorded data, the filter of the transimpedance amplifier was set to about 20 kHz. The field emission circuit noise was recorded prior to the field emission experiments for gains  $10^7$  and  $10^8$  V/A. Fig. 3 shows the noise spectra of the field emission circuit. The noise in the circuit for the gains  $10^7$  and  $10^8$  V/A consists of mainly the harmonics greater than 10 Hz with dominant peaks of about 1 nA at 60 Hz, and the rms of 0.55 nA and 0.51 nA, respectively.

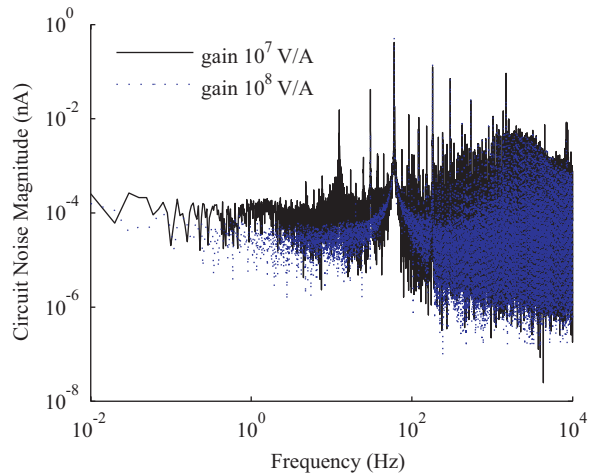


Fig. 3 Noise spectra of field emission circuit

Five emission current measurements lasting five minutes each were recorded with several minutes of separation between each measurement. The first measurement was recorded almost immediately after the emission current reaches about 10 nA. The emission current was then increased to about 100 nA in the following 4 minutes after the first measurement was completed. Then, four measurements of the emission current at about 100 nA were recorded with several minutes between each measurement.

## Result and Discussion

The measured current data is transformed into the frequency domain with a discrete fast Fourier transform (FFT). Fig. 4 illustrates the emission current of measurement#1 with its corresponding spectrum. The emission current is quite stable with occasional fluctuations which consist of the superimposed of the low frequency harmonics that form the spikes. The mean current is 10.2 nA and the rms is 2.4 nA. The dominant peaks of the harmonics greater than 5 Hz occurred at about 12.5, 60, 180, and 5836 Hz.

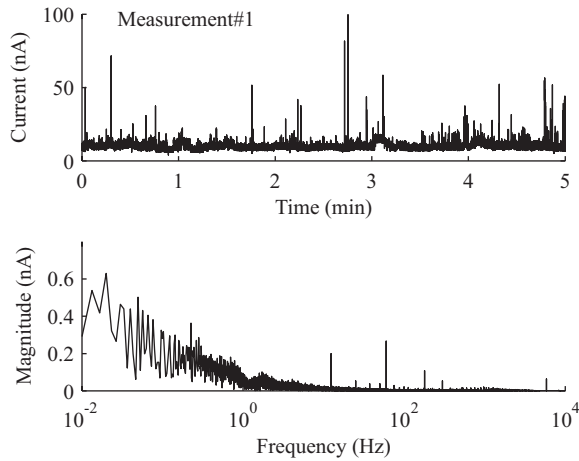


Fig. 4 Measured current and spectrum of measurement#1

Fig. 5 and Fig. 6 show the measured current and the spectra from measurement#2 to #5. The stability in the emission current improves from measurement#2 to measurement#5 after 44 minutes of emission at about 100 nA. The improvement is further indicated by the gradual reduction in the magnitude spectra below about 5 Hz with the exception to measurement#4. The trend maybe associated with the removal of the adsorbates due to resistive heating of the CNT [10]. The higher frequency peaks indicate that the noise in the emission current occurred at 60 and 5840 Hz.

Fig. 7 illustrates the transient (measured) current separated into low frequency (stability) and high frequency (noise) harmonics with the cutoff frequency chosen at 5 Hz. The stability and noise are characterized by considering the shape of the probability density function (PDF). Skewness is a measure of the asymmetry of the data around the sample mean. And, kurtosis is a measure of how outlier-prone (peakedness) a distribution is. Table 1 summaries the statistical parameters such as mean, root-mean-square (rms), skewness, and kurtosis of emission current.

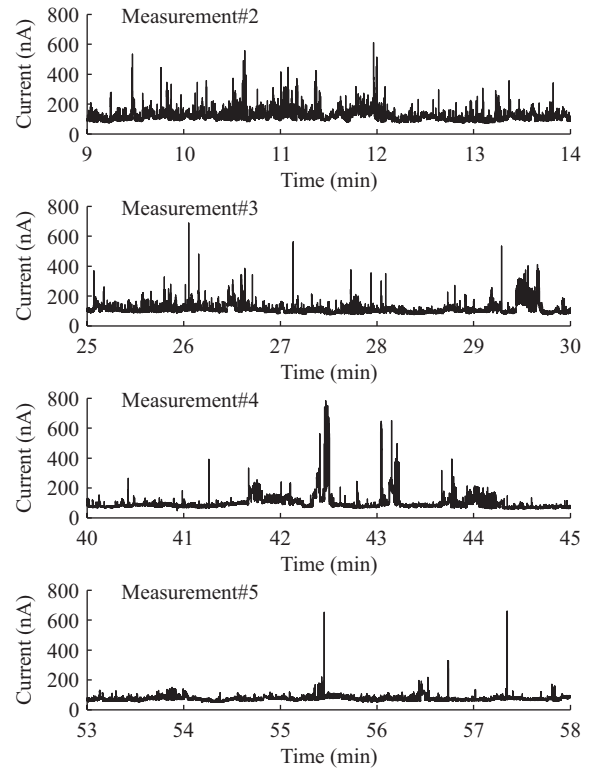


Fig. 5 Measured current for measurement#2 to #5

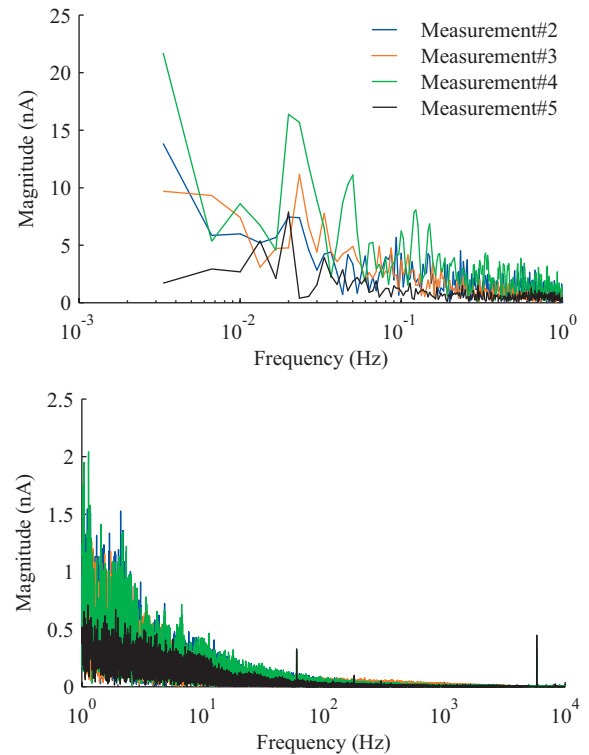


Fig. 6 Spectra of measurement#2 to #5

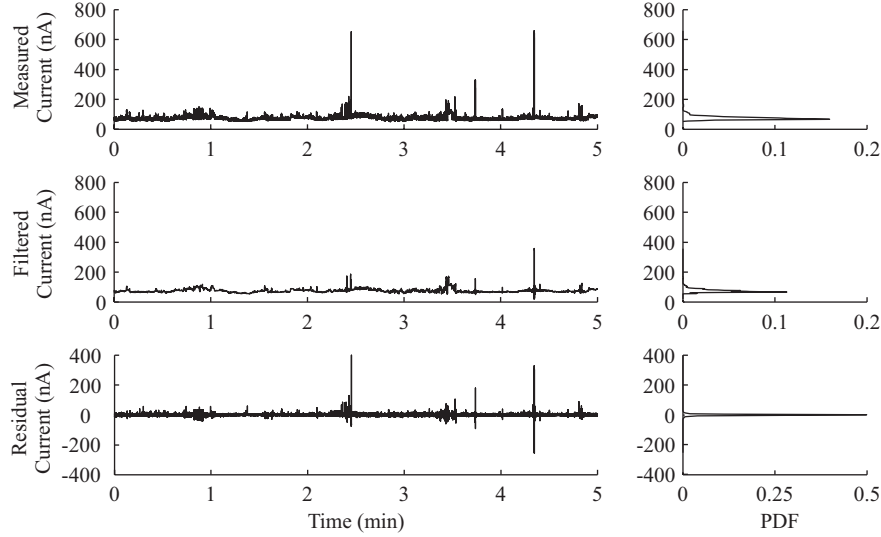


Fig. 7 Separation of measured current into low-frequency component (filtered current) and high-frequency component (residual current) using 5 Hz separation frequency

Table 1. Statistical parameters determined for measured and separated currents

Measurement	Measured current				Filtered current (stability)				Residual current (noise)		
	mean (nA)	rms (nA)	skewness	kurtosis	mean (nA)	rms (nA)	skewness	kurtosis	rms (nA)	skewness	kurtosis
1	10.2	2.4	6.4	77.5	10.2	2.2	6.7	79.0	1.0	2.7	147.7
2	115.5	29.7	2.9	18.6	115.5	27.9	2.6	15.8	10.1	3.7	79.9
3	108.5	27.3	3.7	28.2	108.5	25.3	3.0	18.6	10.2	3.0	71.7
4	96.3	44.8	5.0	39.9	96.3	43.3	4.7	36.6	11.5	4.1	192.2
5	74.5	15.2	10.4	305.4	74.5	13.4	4.4	56.2	7.2	6.7	608.7

## Conclusions

The emission current from CNT field emitters can be analyzed and studied by separating low frequency harmonics as stability (<5 Hz) and high frequency harmonics as noise (>5 Hz) in the frequency domain. The emission current exhibits positive skewness and high kurtosis in all the measurements.

## Acknowledgements

This research is supported by the NSF Nanoscale Interdisciplinary Research Team (NIRT) award from the Nano Manufacturing program in Design, Manufacturing, and Industrial Innovation under Grant No. DMI-0210559.

## References

- [1] W. A. deHeer, W. S. Bacsá, A. Chatelain, T. Gerfin, R. Humphreybaker, L. Forró, and D. Ugarte, *Science* 268, 845 (1995).
- [2] A. G. Rinzler, J. H. Hafner, P. Nikolaev, L. Lou, S. G. Kim, D. Tomanek, P. Nordlander, D. T. Colbert, and R. E. Smalley, *Science* 269, 1550 (1995).
- [3] B. T. Wong, M. P. Mengüç, and R. R. Vallance, *ASME Journal of Heat Transfer* 126, 566 (2004).
- [4] M. J. Fransen, Th. L. van Rooy, and P. Kruit, *Appl. Surf. Sci.* 146, 312 (1999).
- [5] J. C. She, N. S. Xu, S. Z. Deng, J. Chen, H. Bishop, S. E. Huq, L. Wang, D. Y. Zhong, and E. G. Wang, *Appl. Phys. Lett.* 83, 2671 (2003).
- [6] P. W. Hawkes and E. Kasper, *Principle of Electron Optics II: Applied Geometrical Optics* (Academic, London, 1996).
- [7] M. J. Fransen, *Toward high brightness, monochromatic electron sources*, Technische Universiteit Delft, 1998.
- [8] H. Tanaka, S. Akita, L. Pan, and Y. Nakayama, *Jpn. J. Appl. Phys.* 43, 1651 (2004).
- [9] D. W. Tuggle, J. Jian, and L. F. Dong, *Surface and Interface Analysis* 36, 489 (2004).
- [10] K. A. Dean and B. R. Chamala, *Appl. Phys. Lett.* 76, 375 (2000).